Transactions of the Materials Research Society of Japan 30[3] 909-912 (2005)

Atomistic Studies on High-Temperature Elasticity and Auxetic Behavior in SiO_2 Polymorphs

Hajime Kimizuka*,†, Shigenobu Ogata‡,* and Yoji Shibutani*,‡
* Department of Mechanical Engineering, Graduate School of Engineering, Osaka University,
2-1 Yamadaoka, Suita, Osaka 565-0871, Japan
Fax:+81-6-6879-4121, e-mail: kimizuka@comec.mech.eng.osaka-u.ac.jp
† Engineering Technology Division, The Japan Research Institute, Limited, 16 Ichiban-cho, Chiyoda-ku,
Tokyo 102-0082, Japan
‡ Science and Technology Center for Atoms, Molecules and Ions Control, Graduate School of Engineering,
Osaka University, 2-1 Yamadaoka, Suita, Osaka 565-0871, Japan

We have investigated the topological structure of three-dimensional network glass, such as vitreous SiO_2, and its effect on the elastic properties with a molecular-dynamics (MD) approach. The topological analysis based on the graph theory is employed to characterize disordered networks in the model systems of vitreous SiO_2, and thus the results concerning the structure of n-membered rings are presented. The adiabatic elastic constants of vitreous SiO_2 are evaluated at finite temperatures, with the fluctuation formula for the internal stress tensor using the MD method. The quantitative relation between the statistics of rings in vitreous SiO_2 and the elastic properties are studied. In addition, the corresponding MD results for the high-temperature elasticity and auxeticity of crystalline SiO_2, α- and β-cristobalite, are presented for comparison.

Keywords: negative Poisson's ratio, elastic constant, molecular dynamics, cristobalite, vitreous SiO_2

1 INTRODUCTION

One of the most important properties of vitreous SiO_2 is its extremely low coefficient of thermal expansion. This makes the material particularly useful for optical flats, mirrors, furnace windows and critical optical applications which require minimum sensitivity to thermal changes. It is particularly known that devitrification and particle generation due to the nucleation of cristobalite are limiting factors in the high temperature performance of vitreous SiO_2. In order to properly assess the mechanical degradation of vitreous SiO_2 under high-temperature conditions, it is important to understand the elastic behavior of both cristobalite and vitreous SiO_2 over a wide temperature range.

Cristobalite, a low density polymorph of SiO_2, shows an anomalous elastic property of a negative Poisson's ratio [1, 2]. Negative Poisson's ratio materials undergo lateral contraction under longitudinal compression, and also lateral expansion under longitudinal tension, so-called "auxetic" behavior [3]. In cristobalite, the negative Poisson's ratio appears over the entire temperature range of 300-1800 K, where the bulk modulus is extremely low compared with the shear modulus [4]. Markedly different mechanical properties are found between the two silica, including that cristobalite is auxetic whereas the vitreous SiO_2 is not.

Silica exists in a variety of topologically-different crystalline forms, such as quartz, cristobalite, tridymite, coesite, etc. The elementary unit in these polymorphs at ambient pressure is an almost ideal $Si(O_{1/2})_4$ tetrahedron. Their structures are made up of different arrangements of corner-sharing tetrahedral elementary units. Vitreous SiO_2, which is one of the principal network glass-forming systems, has a topologically-disordered network structure and exhibits an amorphous state.

It is believed that many important macroscopic properties of materials, including elastic and mechanical properties, depend on the underlying microscopic structures. The main objective of the present paper is to provide results of the molecular-dynamics (MD) simulations that can be used to investigate the microscopic structures of cristobalite and vitreous SiO_2, and their effect on the macroscopic elastic properties, in particular, the high-temperature elasticity and auxeticity. Using the MD configurations, we also investigate the medium-range order structure of the amorphous state in vitreous SiO_2, such as the n-membered rings and their distribution.

2 COMPUTATIONAL METHOD

To obtain the model system of vitreous SiO_2, equilibrium molecular dynamics (MD) simulations have been performed within the Nosé-Hoover [5, 6] and Parrinello-Rahman [7] isothermal-isobaric ensemble. We start from the model system of α-cristobalite [9], and heat the system gradually from 300 K to 5000 K at the rate of 50 K/ps, after which the system is equilibrated over 80 ps. The integration time step in all MD simulations is 2 fs. The amorphous state is obtained from a well-thermalized molten state at 5000 K by quenching to room temperature 300 K, at the rate of -50 K/ps. In the quenched state, atoms only vibrate around their equilibrium positions, and no diffusion occurs on the time scale of the MD runs. The fluctuation formula for the internal stress tensor [8] is adopted to obtain a complete set of adiabatic elastic constants at finite temperatures. In order to check the validity of statistical sampling, the averages are separately taken every 40 ps during a 0.64 ns run.

We have employed the nonempirical pairwise potential by van Beest, Kramer, and van Santen [10] (BKS), derived from the cluster calculations of potential energy surfaces using the *ab initio* method. This potential has been found to adequately describe a wide scope of properties of SiO_2 through numerous previous studies. Here, to eliminate spurious effect, driven by the dispersion terms which overwhelm all the other terms at very short distances, the original BKS interatomic potential is modified by adding a Lennard-Jones (24-6) contribution [11]. The functional form of the modified version of BKS potential (BKSm) is expressed as

$$\begin{aligned} u(r_{ab}) &= \frac{z_a z_b e^2}{r_{ab}} + a_{ab}\exp(-b_{ab}r_{ab}) - \frac{c_{ab}}{r_{ab}^6} \\ &\quad + 4\epsilon_{ab}\left[\left(\frac{\sigma_{ab}}{r_{ab}}\right)^{24} - \left(\frac{\sigma_{ab}}{r_{ab}}\right)^{6}\right], \qquad (1) \end{aligned}$$

where $u(r_{ab})$ is the interaction energy between the two atoms a and b ($a, b \in \{\mathrm{Si,O}\}$), r_{ab} is the interatomic separation, and (z_a, z_b, a_{ab}, b_{ab}, c_{ab}) are parameters fitted to Hartree-Fock calculations for H_4SiO_4 molecules as basic building blocks of various phases of SiO_2. The force-field parameters and the adjustment parameters (ϵ_{ab} and σ_{ab}) used in this work are given in Refs. [10, 11]. The Coulomb interactions are calculated using the Ewald method.

The number of atoms in the system is 576 (containing 48 unit cells), and we use periodic boundary conditions. To estimate the finite-size effects, the MD calculations are also performed on the 4608- and 36864-atom systems (576×2^3 and 576×4^3, respectively).

3 RESULTS AND DISCUSSION

3.1 Structure of vitreous SiO_2

To characterize the structures of amorphous states from the MD results, the radial distribution functions (RDFs) for O-O distances in crystalline, liquid, and vitreous SiO_2 were calculated (Fig. 1). In Fig. 1, we observe that the first-nearest O-O distance remains essentially unchanged during the heating and quenching of the system (between 300-5000 K), and the rigid $Si(O_{1/2})_4$ tetrahedral units in SiO_2 structure are maintained over the phase transformations. However, the peaks, which indicate medium-range order beyond the nearest neighbors, become much broader and even decay in the amorphous state. This indicates that oxygen sites are less ordered in vitreous SiO_2, and $Si(O_{1/2})_4$ tetrahedral orientations (specified by corner oxygen positions) widely distribute due to the destruction of the long-range periodicity. The profiles for the three vitreous SiO_2 models of different system sizes (from 576 to 36864 atoms) look so similar that they are hardly distinguished each other.

In the network-forming structure such as vitreous SiO_2, it is important to investigate the character and dynamics of the underlying microscopic structures. It is possible to describe the nature of the connectivity of the elementary units, beyond the nearest neighbor, in terms of n-membered rings. Fig. 2 shows the n-membered ring structures of different sizes, where $n = 4$ and 6. They are defined as the closed paths containing n Si-O segments, and black and gray spheres represent silicon and oxygen atoms, respectively. The medium-range order structure in crystalline and disordered networks can be characterized in terms of their ring structures and distributions derived with a shortest-path analysis (see, for example, Ref. [12]). Rings defined by the method are a convenient way to analyze SiO_2-type covalent structures. If a silicon atom has four oxygen nearest neighbors, then there are six O-Si-O paths emanating from each Si atom. Shortest-path analysis involves taking every pair of bonds on each silicon atom in turn and finding the smallest size ring. For a four fold-coordinated network such as SiO_2 at ambient pressure containing N_{Si} silicon atoms, there are $6N_{Si}$ rings. An n-membered ring therefore contains $2n$ Si-O bonds. Using this ring analysis, one finds that cristobalite consists entirely of six-membered rings, whereas quartz has six-membered and eight-membered ring.

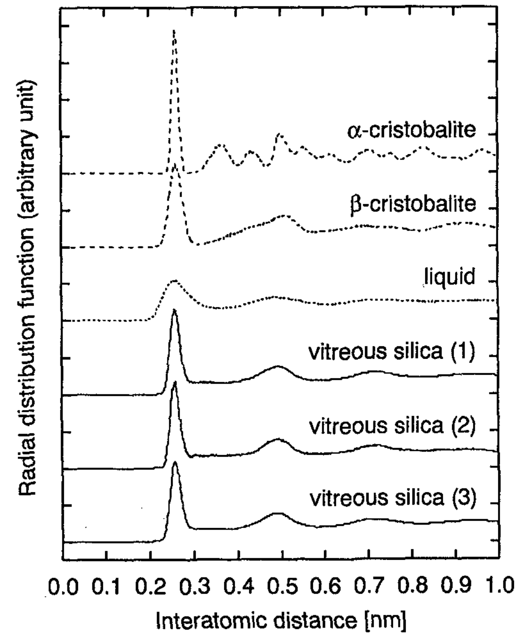

Fig. 1: Radial distribution functions (RDFs) of crystalline, liquid, and vitreous SiO_2 for O-O distance. Solid curves denote the RDFs for the (1) 576-atom, (2) 4608-atom, and (3) 36864-atom systems of vitreous SiO_2, respectively. The RDFs of crystalline (α- and β-cristobalite) and liquid SiO_2 are represented by dashed curves.

Table I shows the statistics of rings of sizes from 2 to 9. The listed values exhibit the population of each ring, normalized by the number of silicon atoms (N_{Si}) in the system. Note that the three systems of vitreous SiO_2 have almost the same ring distribution. In all cases, the distribution is peaked at a six-membered ring, and nearly symmetric around the value. Also, the population of five-membered rings is slightly but

Table I: Statistics of n-membered rings per $Si(O_{1/2})_4$ tetrahedron in vitreous SiO_2.

Ring size (n)	2	3	4	5	6	7	8	9
α- and β-cristobalite					6			
vitreous SiO_2 ($N = 576$)	0.05	0.05	0.68	2.06	2.17	1.27	0.35	0.03
vitreous SiO_2 ($N = 4608$)	0.04	0.09	0.69	1.78	2.16	1.34	0.40	0.04
vitreous SiO_2 ($N = 36864$)	0.05	0.14	0.85	1.90	2.18	1.34	0.39	0.03

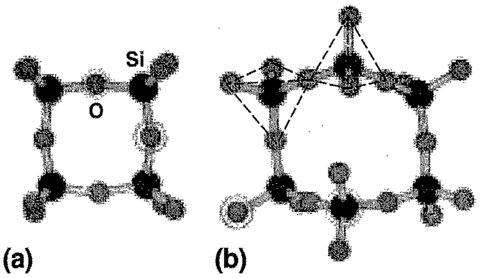

Fig. 2: Examples of n-membered rings for (a) $n = 4$ and (b) $n = 6$. Black and gray spheres represent silicon and oxygen atoms, respectively. Dotted lines within the rings indicate the $Si(O_{1/2})_4$ tetrahedral sub-units.

clearly larger in the 576-atom system, compared with the others. It suggests that the relative populations of rings are not well described in a smaller system, due to the limitation of size.

3.2 Elastic properties of cristobalite and vitreous SiO_2

The adiabatic elastic stiffness constants (C_{ij}) of vitreous SiO_2 were evaluated using the MD simulations with the BKSm potential. The obtained C_{ij} values are given in Table II, for the systems of 576, 4608, and 36864 atoms. We have included the experimental values [1] for comparison, as well as the results of previous MD calculations [4] for α- and β-cristobalite using the original BKS potential.

In the calculations of elastic constants of vitreous SiO_2, we observe the three finite elements, C_{11}, C_{44}, and C_{12}. The three components can be reduced to two based on the equation $C_{44} = \frac{1}{2}(C_{11} - C_{12})$, in the isotropic media such as vitreous SiO_2. In Table II, we confirm that this isotropic solid criterion is well satisfied for the three vitreous SiO_2 models. Also, the bulk component C_{11} is much larger than the shear component C_{44} in vitreous SiO_2, as in ordinary solids, whereas C_{11} is smaller or almost equal to C_{44} in α- and β-cristobalite. This fact suggests that the peculiar effect of microscopic structures on the macroscopic elasticity exits in the crystalline SiO_2 form, cristobalite.

In β-cristobalite, it is noteworthy that the C_{11} exhibits extremely close value to the C_{44}, in contrast to the Cauchy relation. This result is unusual in the ordinal cubic crystals, whereas the well-known Born stability criteria for cubic crystals are well satisfied [4]. Thus we predict that the elasticity of β-cristobalite can be described by only two quantities; however, it clearly differs from the isotropic media such as vitreous SiO_2, as in Table II.

The bulk modulus (K) and shear modulus (G) for an isotropic aggregate of cristobalite and vitreous SiO_2 were evaluated from the C_{ij}'s by means of the Voigt-Reuss-Hill average. Table III shows K, G, and the Poisson's ratios (ν) of the single-phased aggregate of cristobalite and vitreous SiO_2. Here, the sign of a Poisson's ratio is determined by the relationship between K and G, as in the following formula: $\nu = (1/2)(3K - 2G)/(3K + G)$.

In vitreous SiO_2, the bulk modulus is extremely high compared with the shear modulus, and thus the Poisson's ratio exhibits a positive value as in ordinary solids. Also, while the shear modulus exhibits almost the same value in the three amorphous systems, the bulk modulus is clearly different between the 576-atom system and the others. Since these three systems are found to have almost the same density in the MD calculations ($\rho = 2.69$, 2.68, and 2.71 g/cm^2 for the 576-, 4608-, and 36864-atom systems, respectively), it is predicted that this result is due to the difference in the medium-range order structure, especially in the population of five-membered rings. It is suggested that the large population of rings smaller than size 6 brings relatively high incompressibility in SiO_2-type covalent structures, due to the limitation of the cooperative motions of $Si(O_{1/2})_4$ tetrahedra.

In α-cristobalite, the negative Poisson's ratio results from the typical framework structure of α-cristobalite which consists of uniform six-membered rings [1, 4]. These rings have an inverted characteristic similar to re-entrant honeycombs, the typical model which induces a negative Poisson ratio [13, 14]. Here, the bulk modulus is extremely low compared with the shear modulus, as in Table III. We predict that the softening of the bulk modulus in cristobalite occurs due to the cooperative motions of $Si(O_{1/2})_4$ tetrahedra, whereas the anomalous properties are localized due to the destruction of long-range periodicity in vitreous SiO_2.

4 SUMMARY

This paper presents the molecular-dynamics (MD) results concerning the structural and elastic properties of cristobalite and vitreous SiO_2, the typical polymorphs of SiO_2. Using the equilibrium MD method with a stress-fluctuation formula, we have successfully evaluated the adiabatic elastic constants of (α,β)-cristobalite and vitreous SiO_2 at finite temperatures. The nature of connectivity of the elementary units

Table II: Adiabatic elastic constants (in GPa) of cristobalite and vitreous SiO_2.

	α-cristobalite		β-cristobalite	vitreous SiO_2 (300 K)		
	Expt.[a]	BKS[b]	BKS[b]	$N = 576$	$N = 4608$	$N = 36864$
C_{11}	59.4	64.5	49.6	135.3	113.0	120.4
C_{33}	42.4	37.9	—	—	—	—
C_{44}	67.2	69.5	49.7	40.1	41.8	38.8
C_{66}	25.7	27.6	—	—	—	—
C_{12}	3.8	6.5	5.7	44.4	36.7	36.0
C_{13}	−4.4	−0.7	—	—	—	—
$\frac{1}{2}(C_{11} - C_{12})$	—	—	—	45.5	38.2	42.2

[a] Reference [1].
[b] Reference [4].

Table III: Isotropic bulk modulus (K in GPa), shear modulus (G in GPa), and Poisson's ratio (ν) of cristobalite and vitreous SiO_2.

	α-cristobalite		β-cristobalite	vitreous SiO_2 (300 K)		
	Expt.[a]	BKS[b]	BKS[b]	$N = 576$	$N = 4608$	$N = 36864$
K	16.37	18.8	20.3	74.3	61.9	63.9
G	39.05	39.4	35.8	41.9	40.2	39.8
ν	−0.163	−0.12	−0.05	0.26	0.23	0.24

[a] Reference [1].
[b] Reference [4].

beyond the nearest neighbor is characterized in terms of the ring distribution by shortest-path analysis, and the results can be associated with the medium-range order structure of amorphous state in vitreous SiO_2. It is suggested that the microscopic structures in vitreous SiO_2 affect the elastic properties directly. Also, we have investigated the characteristic high-temperature elasticity of cristobalite, using the MD simulations based on the BKS pairwise potentials. We confirm that cristobalite exhibits a negative Poisson's ratio over the wide temperature range of 300-1800 K, whereas vitreous SiO_2 exhibits the positive value at 300 K. To this end, our simulations provide the microscopic insight into the intimate relation between the elastic behavior and the nature of connectivity of the elementary $Si(O_{1/2})_4$ units, in the SiO_2 polymorphs.

ACKNOWLEDGEMENTS

H.K. would like to thank Hideo Kaburaki and Yoshiaki Kogure for their support and encouragements during the research.

REFERENCES

[1] A. Yeganeh-Haeri, D. J. Weidner, and J. B. Parise, *Science* **257**, 650 (1992).

[2] N. R. Keskar and J. R. Chelikowsky, *Nature (London)* **358**, 222 (1992).

[3] K. E. Evans, M. A. Nkansah, I. J. Hutchinson and S. C. Rogers, *Nature (London)* **353**, 124 (1991).

[4] H. Kimizuka, H. Kaburaki, and Y. Kogure, *Phys. Rev. Lett.* **84**, 5548 (2000).

[5] S. Nosé, *Mol. Phys.* **52**, 255 (1984).

[6] W. G. Hoover, *Phys. Rev. A* **31**, 1695 (1985).

[7] M. Parrinello and A. Rahman, *J. Appl. Phys.* **52**, 7182 (1981).

[8] J. R. Ray, M. C. Moody, and A. Rahman, *Phys. Rev. B* **32**, 733 (1985).

[9] J. J. Pluth, J. V. Smith, and J. Jr. Faber, *J. Appl. Phys.* **57**, 1045 (1985).

[10] B. W. H. van Beest, G. J. Kramer, and R. A. van Santen, *Phys. Rev. Lett.* **64**, 1955 (1990).

[11] Y. Guissani and B. Guillot, *J. Chem. Phys.* **104**, 7633 (1996).

[12] J. P. Rino, I. Ebbsjö, R. K. Kalia, A. Nakano, and P. Vashishta, *Phys. Rev. B* **47**, 3053 (1993).

[13] R. F. Almgren, *J. Elasticity*, **15** 427 (1985).

[14] L. J. Gibson and M. F. Ashby, Cellular Solids: Structure & Properties (Pergamon, Oxford, 1988).

(Received December 23, 2004; Accepted April 28, 2005)